

# Asymmetric Construction of Low-Latency and Length-Flexible Polar Codes

Adam Cavatassi, Thibaud Tonnellier and Warren J. Gross

Department of Electrical and Computer Engineering

McGill University, Montréal, Québec, Canada

Email: adam.cavatassi@mail.mcgill.ca, thibaud.tonnellier@mail.mcgill.ca, warren.gross@mcgill.ca

**Abstract**—Polar codes are a class of capacity-achieving error correcting codes that have been selected for use in enhanced mobile broadband in the 3GPP 5<sup>th</sup> generation (5G) wireless standard. Most polar code research examines the original Arıkan polar coding scheme, which is limited in block length to powers of two. This constraint presents a considerable obstacle since practical applications call for all code lengths to be readily available. Puncturing and shortening techniques allow for flexible polar codes, while multi-kernel polar codes produce native code lengths that are powers of two and/or three. In this work, we propose a new low complexity coding scheme called asymmetric polar coding that allows for any arbitrary block length. We present details on the generator matrix, frozen set design, and decoding schedule. Our scheme offers flexible polar code lengths with decoding complexity lower than equivalent state-of-the-art length-compatible approaches under successive cancellation decoding. Further, asymmetric decoding complexity is directly dependent on the codeword length rather than the nearest valid polar code length. We compare our scheme with other length matching techniques, and simulations are presented. Results show that asymmetric polar codes present similar error correction performance to the competing schemes, while dividing the number of SC decoding operations by up to a factor of 2 using the same codeword length.

## I. INTRODUCTION

Polar codes are capacity achieving error-correcting codes [1] that have been selected for control channel use in the 3GPP 5th generation (5G) New Radio standard [2]. Conventional (or Arıkan) polar codes can natively only attain length  $N$  such that  $N = 2^n$  with  $n \in \mathbb{N}^+$ . The generator matrix of an Arıkan polar code is obtained by applying the  $n$ -th Kronecker product, denoted as  $\otimes$ , on the Arıkan kernel  $T_2 = \begin{bmatrix} 1 & 0 \\ 1 & 1 \end{bmatrix}$ , resulting in an  $N \times N$  matrix. However, length-flexible codes are mandatory for practical communication systems. LDPC codes were favoured for the data channel in 3GPP New Radio due to their length flexibility and their decoding complexity, which is directly linked to their codeword size [3]. Thus far, multiple promising schemes have been proposed to assuage the length restriction of polar codes: puncturing [4] and shortening [5] (PS) and multi-kernel (MK) polar codes [6]. Chained polar subcodes [7] were shown to be an effective method for achieving length compatible polar codes, although their complexity precludes their practicality and thus are out of the scope of this paper.

Several PS schemes have been introduced whereby the encoding of a block length of size  $N_P$  is realized by considering a length  $2^{N_M}$  mother polar code where  $N_M = \lceil \log_2 N_P \rceil$ .

Then,  $2^{N_M} - N_P$  bits are either shortened or punctured and are not transmitted over the channel. Decoding is then enacted on the mother code. PS patterns have an impact on bit reliabilities, and so code construction must be co-optimized with the PS sets. Such complications can be neglected with the low complexity methods proposed in [8]. Furthermore, the decoding computational complexity of PS schemes is dependent on that of the mother code.

MK codes [6], [9] are a technique that combines differently sized kernels. Although larger sizes are possible, kernels sizes 2 and 3 are most common, allowing any block length  $N_{MK} = 2^n 3^m$  to be obtained. MK codes offer improved native length flexibility over Arıkan polar codes, though they introduce further complexity to decoding and code design [10].

In this paper, we propose a new coding scheme in which polar codes of unequal lengths are linked together using polar transformations. We refer to the new codes as asymmetric polar codes (APC). By linking multiple polar codes together, any arbitrary block length can be achieved. Our method offers a straightforward approach to polar coding that is length-flexible and exhibits length-dependent decoding complexity. APCs are similar to Arıkan polar codes in the sense that they both have a recursive structure and contain smaller polar codes in their generator matrix. Many previously designed polar decoders and construction methods for Arıkan codes are applicable to APCs. Notably, APCs feature reduced time and space complexity with comparable frame error rate (FER) performance to equivalent PS codes. APCs also have inherently reduced decoding latency against PS codes due to the sequential nature of successive cancellation.

The remainder of this paper is organized as follows: Section II reviews polar code preliminaries, and existing length compatible polar code principles. In Section III, asymmetric polar codes are introduced, including details on encoding, decoding, and code construction. In Section IV experimental results are provided both in terms of decoding performance and complexity evaluation.

## II. POLAR CODES

### A. Generator Matrix Construction

A polar code, denoted by  $\mathcal{PC}(N, K)$ , is a linear block code of length  $N$  and rate  $R = \frac{K}{N}$ . Channel polarization causes individual bit indices to act as synthetic subchannels with either a higher or lower reliability than the original uncoded

channel [1]. Among the  $N$  sub-channels, the first  $K$  indices from  $\mathcal{R}$ , an index vector sorted by reliability, constitute the information set  $\mathcal{I}$  to transmit data. The  $N - K$  remaining positions comprise the frozen set  $\mathcal{F}$  and are typically set to 0.

The uncoded input vector can be written as  $\mathbf{u} = (u_0, u_1, \dots, u_{N-1})$ , and the polar codeword is obtained with  $\mathbf{x} = \mathbf{u}\mathbf{G}_N$ , where the generator matrix  $\mathbf{G}_N = \mathbf{T}_2^{\otimes n}$ . A key property of polar codes is that the encoder is recursive. As such, the generator matrix of a code of length  $N = 2^n$  contains in it all smaller polar codes of length  $N = 2^{n-1}, 2^{n-2}$ , etc. Codeword  $\mathbf{x}$  is transmitted over channel  $W$  and received as vector of log likelihood ratios (LLR)  $\mathbf{y}$ . References to Arkan polar codes in this paper will indicate this construction.

### B. Decoding

The fundamental decoder for polar codes is known as successive cancellation (SC), which was proposed in [1]. It can be viewed as binary tree traversal with left-node-first priority. The noisy codeword  $\mathbf{y}$  is the decoder input at the top of the tree, corresponding to tree stage  $d = n$ . Each node  $v$  contains  $N_v = 2^d$  LLRs  $\alpha$  and bit partial sums  $\beta$ . At each node, the left and right children LLRs,  $\alpha^l$  and  $\alpha^r$ , are computed using  $f$  and  $g$ , respectively:

$$\begin{aligned} \alpha_i^l &= f(\alpha_i, \alpha_{i+\frac{N_v}{2}}) = \alpha_i \boxplus \alpha_{i+\frac{N_v}{2}}, \\ \alpha_i^r &= g(\alpha_i, \alpha_{i+\frac{N_v}{2}}, \beta_i^l) = (-1)^{\beta_i^l} \cdot \alpha_i + \alpha_{i+\frac{N_v}{2}}, \end{aligned} \quad \forall i \in [0, \frac{N_v}{2} - 1] \quad (1)$$

where  $a \boxplus b \approx \text{sign}(a) \text{sign}(b) \min(|a|, |b|)$ . The  $HD$  function is used for computing the bit decision at each leaf node as:

$$\hat{u}_i = HD(\alpha_i) = \begin{cases} 0 & \text{if } \alpha_i > 0 \text{ or } i \in \mathcal{F} \\ 1 & \text{otherwise.} \end{cases} \quad (2)$$

After returning from a right branch, the partial sums in the parent node are updated with  $h(\beta_i, \beta_{i+\frac{N_v}{2}}) = (\beta_i^l \oplus \beta_i^r, \beta_i^r)$  before exploring another branch. Ostensibly, an SC decoder can be reduced to a schedule of  $f$  and  $g$  functions, where the total number of  $f$  and  $g$  operations is given by  $N \log_2 N$ .

To overcome mediocre error rate performance of SC, SC List (SCL) has been proposed in [11]. In the SCL case, each leaf node considers both possible bit values (0 and 1).  $L$  different decoding paths are maintained using a candidate competition based on a path metric, which dictates the pruned paths. SCL becomes more powerful when a CRC (SCL-CRC) is concatenated before polar encoding to aid in path candidate selection. SC and SCL are further enhanced by latency reduction using Fast-SSC [12] [13], which exploits frozen bit locations to identify specialized nodes.

### C. Punctured and Shortened Polar Codes

The standard methods for attaining length compatible polar codes are known as puncturing [4] and shortening [5]. To build a polar code of arbitrary length  $N_S$ , both methods involve freezing additional bits of a larger polar code of length  $N_M = 2^{\lceil \log_2 N_S \rceil}$  to rectify the length difference. This *mother* polar code is used for encoding and decoding. In the case of shortening,  $S = N_M - N_S$  bits in  $\mathbf{u}$  are set to 0, such that the

corresponding indices in  $\mathbf{x}$  are known to be 0. These indices are said to be *overcapable* and are added to the shortening set  $\mathcal{S}$ . To encode,  $\mathcal{S}$  must be included in  $\mathcal{F}$ . Indices in  $\mathcal{S}$  are not transmitted over the channel, and  $\mathcal{S}$  must be known at the decoder. Since shortened indices are known to be 0, their LLRs are set to infinity, or a sufficiently large value in practice, prior to decoding.

Similarly, puncturing  $P = N_M - N_P$  bits allows construction of a code of length  $N_P < N_M$  from a mother code.  $\mathbf{P}$  contains  $P$  *incapable* indices that are added to  $\mathcal{F}$  and not transmitted. Incapable indices are those that are completely unreliable at their leaf node when the corresponding channel value is unreliable during decoding, *ie.*  $\alpha_i = 0$  when  $y_i = 0$  [8]. LLRs of these indices are treated as erasures and set to 0 before the decoder is enacted.

The Wang-Liu (WL) [5] method for shortening and quasi-uniform puncturing (QUP) [4] produce frozen sets that weigh the modified reliabilities of punctured and shortened bits. As such, these methods require reliability computation after the sets  $\mathbf{P}$  or  $\mathcal{S}$  are decided. The frozen set must then be redesigned for every length. Bit reversal schemes were proposed to eliminate the optimization overhead of WL/QUP and produce good results [8]. Shortening typically exhibits superior performance to puncturing in high code rates, while the opposite is true for low code rates. In this paper, we will only consider the WL and QUP methods in our evaluation, as these methods are generally superior to the low-complexity methods in terms of error correction performance [8].

### D. Multi-Kernel Polar Codes

MK polar codes were introduced in [6] as an alternative polarizing construction to attain polar codes of lengths other than powers of 2. The ternary kernel  $\mathbf{T}_3 = \begin{bmatrix} 1 & 1 & 1 \\ 1 & 0 & 1 \\ 0 & 1 & 1 \end{bmatrix}$ , was proposed and shown to be optimal in its polarizing effects [9]. It can be used as a Kronecker product component in conjunction with the Arkan kernel, to produce polar codes of length  $N_{MK} = 2^n 3^m$  for  $n, m \in \mathbb{N}$ . The native length flexibility of polar codes is thus improved, however encoding and decoding becomes more convoluted. SC decoding is modified in ternary stages by computing three branches  $\alpha^l$ ,  $\alpha^c$ , and  $\alpha^r$  for each node:

$$\begin{aligned} \alpha_i^l &= \alpha_i \boxplus \alpha_{i+\frac{N_v}{3}} \boxplus \alpha_{i+\frac{2N_v}{3}}, \\ \alpha_i^c &= (-1)^{\beta_i^l} \cdot \alpha_i + \alpha_{i+\frac{N_v}{3}} \boxplus \alpha_{i+\frac{2N_v}{3}}, \\ \alpha_i^r &= (-1)^{\beta_i^l} \cdot \alpha_{i+\frac{N_v}{3}} + (-1)^{\beta_i^l \otimes \beta_i^c} \cdot \alpha_{i+\frac{2N_v}{3}}. \end{aligned} \quad (3)$$

$\beta$  in ternary stages are updated with  $h_3(\beta_i, \beta_{i+\frac{N_v}{3}}, \beta_{i+\frac{2N_v}{3}}) = (\beta_i^l \oplus \beta_i^c, \beta_i^l \oplus \beta_i^r, \beta_i^l \oplus \beta_i^c \oplus \beta_i^r)$ . MK codes introduce complexity by compelling optimization and storage of the kernel order. For example, a code of length  $N_{MK} = 6$  can be built with either Kronecker products  $\mathbf{T}_2 \otimes \mathbf{T}_3$  or  $\mathbf{T}_3 \otimes \mathbf{T}_2$ , which will result in two unique generator matrices. The number of SC decoding operations for MK codes is given by  $N_{MK}(n + m)$ . All instances of MK codes for the remainder of this paper refer to polar code constructions utilizing  $\mathbf{T}_2$  and  $\mathbf{T}_3$  only.

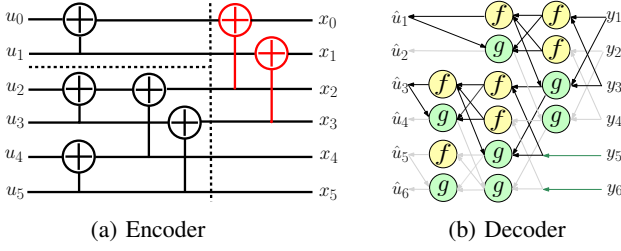


Fig. 1: An *ascending* APC of length  $N_A = 6$  where  $\mathbf{N} = \{4, 2\}$  and  $p = 2$ .

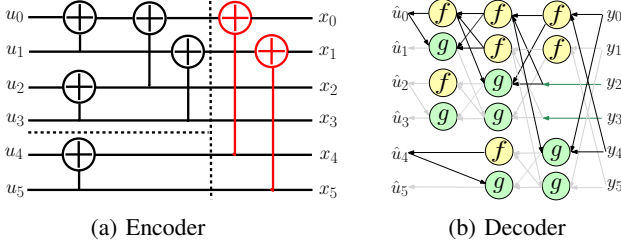


Fig. 2: A *descending* APC of length  $N_A = 6$  where  $\mathbf{N} = \{2, 4\}$  and  $p = 2$ .

### III. LOW LATENCY LENGTH COMPATIBLE POLAR CODES

In this section, we propose a new flexible polar coding scheme called asymmetric polar codes. Commonly researched topics in polar codes such as decoders, construction methods, or hardware implementations can apply to APCs with only some modifications in scheduling.

#### A. Generator Matrix Construction

An APC of length  $N_A$  is constructed from a minimum  $p$  partial polar codes, which are determined by the decomposition of  $N_A$  into a sum of powers of 2, which encompasses the vector  $\mathbf{N} = \{N_0, N_1, \dots, N_{p-1}\}$ . For example, a code length of  $N_A = 14$  is represented in binary as  $1110_2$ , and therefore  $\mathbf{N} = \{8, 4, 2\}$  and  $p = 3$ .  $\mathbf{N}$  can be ordered so that APCs be constructed in either an *ascending* ( $asc = 1$ ) or *descending* ( $asc = 0$ ) permutation. The ascending order indicates that the size of the partial codes increases with bit indices, as in Fig. 1a. Alternatively, the descending order follows that the partial code sizes decrease with bit indices, which requires that  $\mathbf{N}$  be reversed, as in Fig. 2a. The linking process is executed recursively whereby each partial code  $G_{N_l}$  is linked with the next partial code  $G_{N_{l+1}}$  according to the sequence  $\mathbf{N}$ . Generator matrix assembly for APCs requires  $p - 1$  iterations of this process. The polarizing stage used for each iteration  $l$  is the same XOR operation that is used for the last stage of an Arkan code of length  $2N_{l+1}$ . This stage will include  $J_l = \min(\sum_{k=0}^{l+1} N_k - N_{l+1}, N_{l+1})$  sum junctions, detailed in Fig. 3a, which join indices  $j$  and  $j + N_{l+1}$  for  $j \in [0, J_l - 1]$ . The generator matrix  $G_{N_A}$  is equal to the final iteration of the linking matrix, such that  $G_{N_A} = L_{p-2}$ , where  $L_l$  is defined in eq. 4. where  $\hat{\mathbf{1}}_k$  is the all-one vector of length  $k$ , and  $\mathbf{G}[a; \cdot]$  is generator matrix  $\mathbf{G}$  with only its first  $a$  rows. It should be noted that  $\mathbf{N}$  can contain a code length of 1, which equates to a single uncoded bit, *ie.*  $G_1 = [1]$ . Observe that the linking matrix closely resembles the Arkan kernel where  $l > 0$ . Further, this representation makes it possible to obtain

$$L_l = \begin{cases} G_{N_l} & l = 0 \\ \left[ \begin{array}{c|c} G_{N_l} & \mathbf{0} \\ \hline G_{N_l} \otimes \hat{\mathbf{1}}_{\sum_{j<l} N_j} & L_{l-1} \end{array} \right] & l > 0, asc = 1 \\ \left[ \begin{array}{c|c} G_{N_l} & \mathbf{0} \\ \hline G_{N_l} [\sum_{j<l} N_j; \cdot] & L_{l-1} \end{array} \right] & l > 0, asc = 0, \end{cases} \quad (4)$$

Arkan polar codes when  $\mathbf{N}$  contains only two equal lengths. We will only consider the two permutations of  $\mathbf{N}$  using the minimum required partial polar codes in our analysis.

#### B. Example: $N_A = 6$

Observe in Fig. 1a that an encoder with  $N_A = 6$  has constituent polar codes of length 2 and 4. Combining these two partial codes is done with an additional polarizing stage. The additional stage is the same as the last stage of an Arkan polar code of length twice that of the upper code in the Tanner graph. In particular, the upper code in this example has length 2 and thus requires the last stage of a polar code of length 4. The SC decoding schedule must be modified to match the new Tanner graph, as in Fig. 1b.

An APC generator matrix  $G_{N_A}$  must contain those of the constituent codes so as to be consistent with the original polar code definition. Thus,  $G_{N_A}$  is a block matrix comprised of the partial code matrices and the additional polarizing transforms discussed above. In this case, the final ascending matrix  $G_6^{\text{ASC}}$  in eq. (5) has block components  $G_2$  (upper left) and  $G_4$  (lower right) that follow the  $G_N$  definition in Section II-A. Similarly, the descending matrix  $G_6^{\text{DES}}$  is also presented in eq. (5).

$$G_6^{\text{ASC}} = \begin{bmatrix} 1 & 0 & | & 0 & 0 & 0 & 0 \\ 1 & 1 & | & 0 & 0 & 0 & 0 \\ \hline 1 & 0 & | & 1 & 0 & 0 & 0 \\ 1 & 1 & | & 1 & 1 & 0 & 0 \\ 1 & 0 & | & 1 & 0 & 1 & 0 \\ 1 & 1 & | & 1 & 1 & 1 & 1 \end{bmatrix} \quad G_6^{\text{DES}} = \begin{bmatrix} 1 & 0 & 0 & 0 & | & 0 & 0 & 0 \\ 1 & 1 & 0 & 0 & | & 0 & 0 & 0 \\ \hline 1 & 0 & 1 & 0 & | & 0 & 0 & 0 \\ 1 & 1 & 1 & 0 & | & 0 & 0 & 0 \\ 1 & 1 & 1 & 1 & | & 0 & 0 & 0 \\ \hline 1 & 0 & 0 & 0 & | & 1 & 0 & 0 \\ 1 & 1 & 0 & 0 & | & 1 & 1 & 1 \end{bmatrix} \quad (5)$$

#### C. Frozen Set Construction

Most code construction algorithms used to build reliability sets for Arkan codes can be adapted to APCs with minor adjustments. Gaussian approximation [14] (GA) serves as an effective method for designing frozen sets. One must consider the asymmetry of the Tanner graphs of APCs in order to carry out the algorithm accurately. GA entails tracking the reliability of each bit at each stage of the encoder, where the reliabilities are represented by the mean of the LLRs of the synthetic channel. To begin, each coded bit in the encoder is assigned the LLR mean of the uncoded channel  $z = 4R\mathcal{M} \frac{E_b}{N_0}$ , where  $\mathcal{M}$  is the modulation order. The reliabilities are transformed at each summation junction between stage  $d$  and  $d-1$ , as seen in Fig. 3a, according to

$$\begin{aligned} z_0^{d-1} &= \phi^{-1}(1 - (1 - \phi(z_0^d))(1 - \phi(z_1^d))), \\ z_1^{d-1} &= z_0^d + z_1^d, \end{aligned} \quad (6)$$

where  $\phi(x)$  and  $\phi^{-1}(x)$  can be Trifinov's exact formulas [14], or approximations from the open source simulation

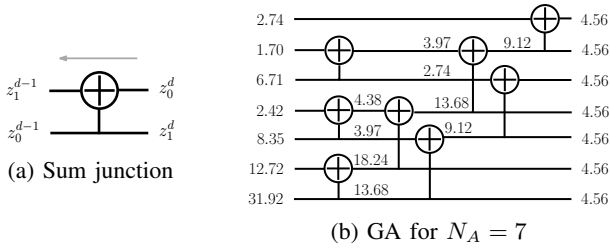


Fig. 3: Gaussian approximation reliability ordering of an ascending asymmetric polar code of length  $N_A = 7$  with  $\mathbf{N} = \{4, 2, 1\}$ .

tool *aff3ct* [15]. Eq. 6 differs from the original GA method in that it cannot assume that each junction input has been transformed equally. Computing the entire graph results in vector of subchannel reliabilities, which serves as a basis to rank indices and form  $\mathcal{R}$ . A construction example for  $\mathcal{PC}(7, 4)$  with  $\mathbf{N} = \{4, 2, 1\}$  is now presented for a target  $\frac{E_b}{N_0} = 3\text{dB}$  where  $W$  is an AWGN channel using BPSK modulation. The full propagation is detailed in Fig. 3b. In this case,  $\mathcal{R} = \{6, 5, 4, 2, 0, 3, 1\}$ ,  $\mathcal{I} = \{6, 5, 4, 2\}$ , and  $\mathcal{F} = \{0, 3, 1\}$ .

#### D. Decoding

Just as when decoding Arkan codes, the operations  $f$  and  $g$  from eq. (1) are used for decoding APCs since the same polarizing transform is used. As such, all standard polar decoders can be used with only a change in schedule according to the new Tanner graph. The SC decoding tree has  $p$  partial code trees that are children of asymmetric nodes and are decoded in the same manner as described in Section II-B. The  $p - 1$  asymmetric nodes are decoded with a schedule that corresponds to the additional polarizing stages outlined in Section III-A. Specifically, each sum junction corresponds to an  $f$  and  $g$  function with equivalent indexing.

The number of computations required by an asymmetric SC decoder is at most  $\sum_{l=0}^{p-1} N_l \log_2 N_l + \sum_{l=1}^{p-1} 2N_l$ , which is proven in the Appendix to be always less than equivalent PS codes, namely  $N_M \log_2 N_M$  where  $N_M = \lceil \log_2 N_A \rceil$ . In the case where  $p \leq 2$ , the ascending and descending APCs have the same number of decoding operations. Generally, the descending permutation requires a higher number of operations.

Fast-SSC decoding schedules can be obtained for APCs since all symmetric nodes remain powers of 2. The SC tree for an ascending APC where  $N_A = 14$ , along with its Fast-SSC counterpart, can be seen in Fig. 4. Regarding error correction performance, the theoretical FER under SC decoding for APCs can be analytically computed using GA bit reliabilities, as was observed for Arkan polar codes in [16, eq. (3)].

### IV. NUMERICAL ILLUSTRATIONS AND ANALYSIS

#### A. Decoding Performance

The error correction capabilities of APCs has been evaluated through a series of simulations using the AWGN channel and BPSK modulation. FER curves have been obtained for  $N \in \{576, 768, 1536, 2304, 3072\}$  and  $R \in \{\frac{1}{4}, \frac{1}{2}, \frac{3}{4}\}$ . SCL-CRC is the decoding algorithm used with list size  $L = 8$  and CRC size 16 using polynomial  $0 \times 1021$ . All frozen sets

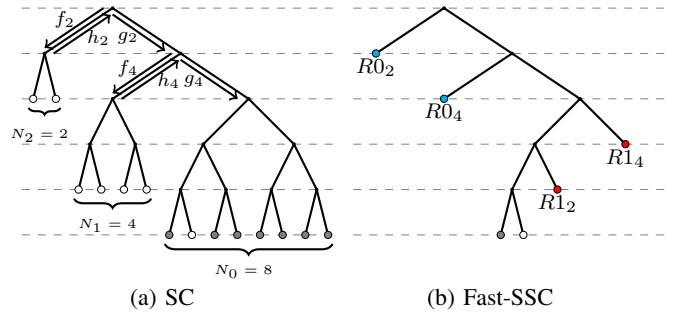


Fig. 4: SC tree for an ascending asymmetric polar code with  $N_A = 14$  and  $\mathbf{N} = \{8, 4, 2\}$ . White, blue, and red leaves are frozen bits, Rate-0 nodes, and Rate-1 nodes, respectively. Subscripts indicate node or function size.

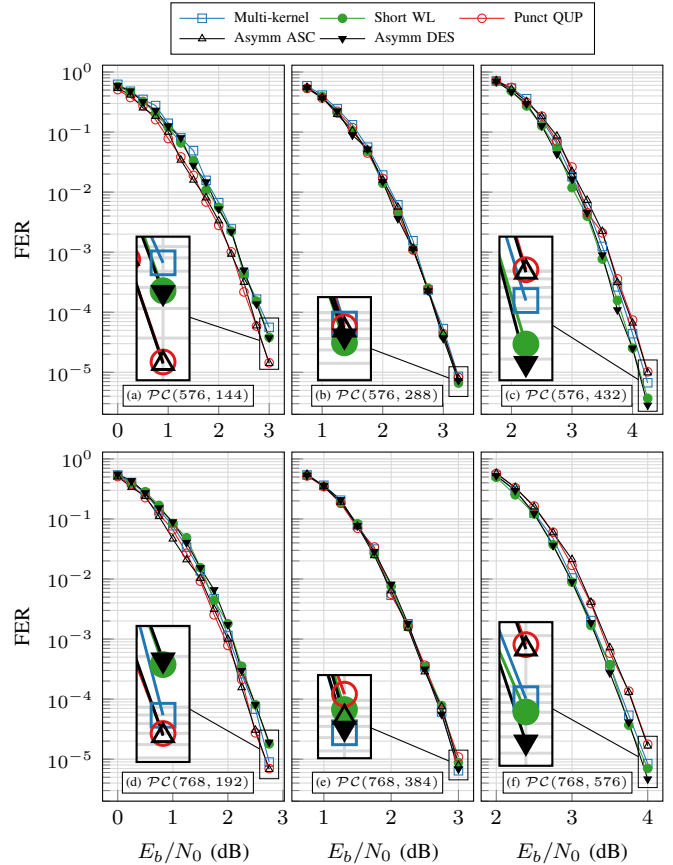


Fig. 5: FER curves for polar codes with  $N \in \{576, 768\}$  (top to bottom) with rates  $R \in \{\frac{1}{4}, \frac{1}{2}, \frac{3}{4}\}$  (left to right).

were reconstructed for each  $\frac{E_b}{N_0}$  value in the plots using GA. We compared APCs with two key PS schemes as well as with MK polar codes. The kernel order of the MK codes was optimized for highest overall reliability by an exhaustive search, as proposed in [6].

Under SCL-CRC decoding, asymmetric codes have comparable performance to leading length-compatible schemes

Scheme	$N = 576$	$N = 768$	$N = 1536$	$N = 2304$	$N = 3072$
APC	5120	7168	15872	25088	34816
PS	10240	10240	22528	49152	49152
MK	4608	6912	15360	23040	33792

TABLE I: Number of SC decoding operations.

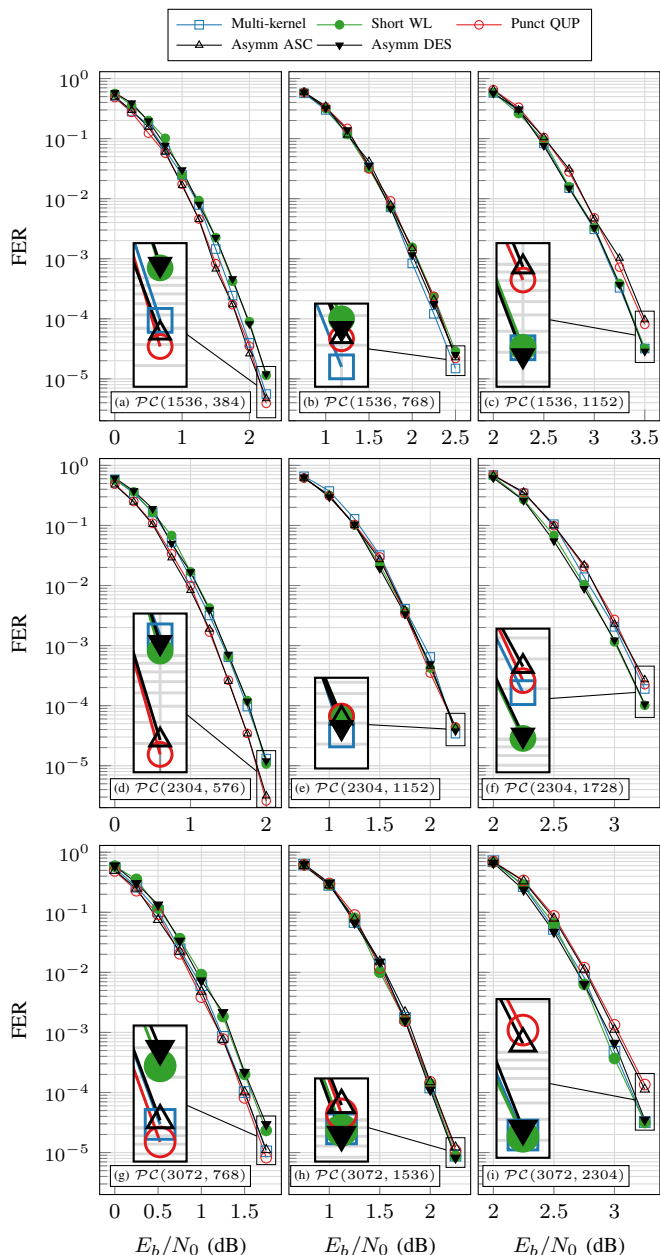


Fig. 6: FER curves for polar codes with  $N \in \{1536, 2304, 3072\}$  (top to bottom) with rates  $R \in \{\frac{1}{4}, \frac{1}{2}, \frac{3}{4}\}$  (left to right).

when using a range of code rates, as depicted in Figs. 5 and 6. In all cases considered, APC performance is in the approximate range of  $[-0.05\text{dB}, +0.05\text{dB}]$  compared to the best performing state-of-the-art codes for  $\text{FER} = 10^{-4}$ . Just as with Arkan polar codes, APC error correction performance generally improves with length. It should be noted that APCs excel when they contain fewer and larger partial polar codes.

For all code lengths, APCs built with the ascending partial code permutation have superior error correction performance to APCs utilizing the descending permutation at low rates, while the opposite is true for high rates. This is due to the fact that the reliability of partial codes is related not only to their location in the Tanner graph, but also their size. Further, APCs have reduced performance when indices

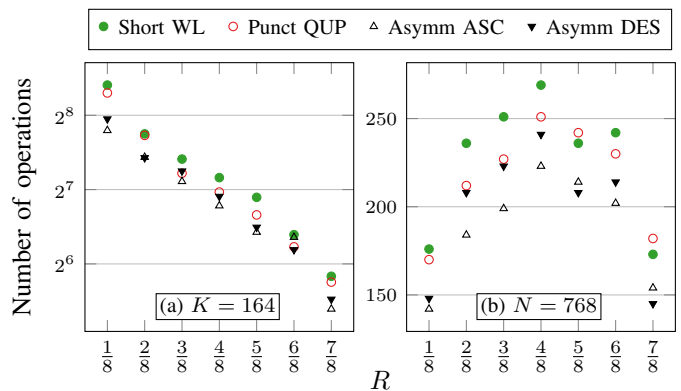


Fig. 7: Fast-SSC complexity with a maximum processor size of 64.

in  $\mathcal{I}$  are found in smaller partial codes. The small partial codes in the descending permutation are where the few highly reliable indices are located at low rates, and so these bits exhibit reduced polarization effects due to the smaller partial code size. Conversely, the ascending permutation allows most information bits to be located in the largest partial codes at low rates, which present the highest reliability. It should also be noted that ascending and descending APCs have very similar performance to punctured and shortened polar codes, respectively. MK codes generally do not outperform PS or APC schemes in the tested scenarios. However, they are more likely to have worse performance when they have more than one ternary stage, as seen in Figs. 5ac and 6df.

### B. Complexity Evaluation

We will analyze the complexity of APCs by comparing them with PS and MK schemes in terms of SC and Fast-SSC decoding complexity, space complexity, and code design. We measured the SC time complexity of all considered techniques by examining the number of LLR operations required for decoding a single codeword. The number of operations required for each scheme is given in Sections II-B, II-D, and III-D. Table I outlines the number of decoding operations required for each simulated case. Observe that both APC and MK codes have comparable decoding complexity that is directly related to their block length. Although MK codes have reduced time complexity over equivalent PS and APC codes, MK decoding requires concessions for ternary decoding using eq. (3), and kernel order in scheduling. The logic required for practical MK implementations is more complex and demands specialized hardware and increased memory over Arkan codes [10]. Further, MK codes are limited in their length flexibility without considering the use of higher order kernels, which introduces further complication. As such, MK complexity is difficult to compare with that of APCs or PS codes.

Comparing Fast-SSC decoding complexity requires a more refined metric. Since there are no fast decoders currently available for MK codes, they will be excluded from this comparison. It was shown in [17] that a processing element size of 64 permits an acceptable balance between decoder throughput and hardware utilization for Arkan polar codes with block length  $N = 1024$ . We will use this baseline

for our comparisons, seeing that our experiments operate on a similar order of magnitude. Given that specialized nodes such as Rate-1, Rate-0, Single-Parity Check, and Repetition [12] are available with a maximum node size of 64, each specialized node is considered a single operation. Additionally, all computations of  $\alpha^l$  and  $\alpha^r$  of children nodes are counted as  $\lceil \frac{N_v}{64} \rceil$  operation(s), where  $N_v$  is the child node size. It is worth noting that PS decoders are likely to have a higher number of Rate-0 and Repetition nodes due to their higher proportion of frozen bits. However, Fig. 7 demonstrates that APCs have between [2.7%, 27%] time complexity reduction under Fast-SSC decoding when compared against PS schemes over a range of block lengths and rates. The degree to which APC complexity is reduced is dependent on the difference between the transmitted block length and the size of the PS mother code. When  $N$  is slightly larger than a power of 2, APCs exhibit higher complexity reduction.

Regarding space complexity, APCs have the smaller memory requirements than PS schemes. Using the efficient SC implementations proposed in [17], APCs only require  $\alpha$  and  $\beta$  memory for the largest partial code, which is at most half that of equivalent PS codes. For example, when  $N = 2304$ , PS decoders require the same  $\alpha$  and  $\beta$  storage capacity as an Arkan code of  $N = 4096$ , while APCs can be decoded with just the memory capacity of a  $N = 2048$  Arkan code and extended channel memory. Conclusively, PS approaches are not an efficient use of time and space resources since they must decode their mother code in order to receive an effectively smaller codeword. Further, MK codes necessitate ternary  $\beta$  memory, which results in increased storage requirements over purely Arkan decoders [10].

Regarding the code construction, MK schemes must optimize the kernel order to maximize performance, and PS schemes must build a reliability set after the PS sets are determined, or vice versa. Thus, APCs demand only a single-step frozen set construction, while the competing schemes call for further considerations.

## V. CONCLUSION

In this work, we introduced the concept of *asymmetric polar codes* and presented techniques to retain known decoders and construction methods. We analyzed our APC construction and evaluated its utility in terms of FER performance and decoding complexity. We compared APCs with state of the art PS and MK codes through simulation. We have demonstrated that APCs are a flexible polar coding scheme that exhibit block length-dependent decoding complexity with similar error correction performance to the state-of-the-art. We established that APCs are a practical family to be added to the polar code tool box. Future work in APCs will involve flexible HARQ retransmission schemes and low complexity frozen set design.

## APPENDIX

*Proof of reduced decoding complexity:* We will show that APCs always require fewer computations than an equivalent

PS code by examining the worst case scenario: when  $asc = 0$  and  $N = 2^p - 1$ . This case yields the highest possible  $p$ . If

$$\sum_{l=0}^{p-1} N_l \log_2 N_l + \sum_{l=1}^{p-1} 2N_l < 2^{\lceil \log_2 N \rceil} \log_2 2^{\lceil \log_2 N \rceil},$$

is true in the worst case, then APCs always require fewer decoding operations than an equivalent PS code for any  $N$ . In this case,  $p = \lceil \log_2 N \rceil = \log_2(N + 1)$  and  $\mathbf{N}$  contains all powers of two less than  $N_M$ :

$$\begin{aligned} \sum_{l=0}^{p-1} 2^l \log_2 2^l + \sum_{l=1}^{p-1} 2 \cdot 2^l &< 2^p \log_2 2^p, \\ \sum_{l=0}^{p-1} l \cdot 2^l + \sum_{l=1}^{p-1} 2 \cdot 2^l &< p \cdot 2^p, \\ p \cdot 2^p - 2 &< p \cdot 2^p. \end{aligned}$$

Thus, APCs have lower decoding complexity than PS codes. It can be shown that APCs have fewer decoding operations when  $asc = 1$  than when  $asc = 0$  by replacing the second summation term with  $\sum_{l=1}^{p-1} 2 \cdot 2^{l-1}$ , which results in a maximum number of decoding operations of  $p \cdot 2^p - 2^p < p \cdot 2^p$ .

## REFERENCES

- [1] E. Arıkan, "Channel Polarization: A Method for Constructing Capacity-Achieving Codes for Symmetric Binary-Input Memoryless Channels," *IEEE Trans. on Inform. Theory*, vol. 55, no. 7, pp. 3051–3073, Jul. 2009.
- [2] 3GPP, "NR; Multiplexing and Channel Coding," <http://www.3gpp.org/DynaReport/38-series.htm>, Tech. Rep. TS 38.212, June 2018, Release 15.
- [3] T. Richardson and S. Kudekar, "Design of Low-Density Parity Check Codes for 5G New Radio," *IEEE Communications Magazine*, vol. 56, no. 3, pp. 28–34, Mar. 2018.
- [4] K. Niu, K. Chen, and J.-R. Lin, "Beyond Turbo Codes: Rate-Compatible Punctured Polar Codes," in *2013 IEEE Int. Conf. Commun. (ICC)*, 2013.
- [5] R. Wang and R. Liu, "A Novel Puncturing Scheme for Polar Codes," *IEEE Commun. Lett.*, vol. 18, no. 12, pp. 2081–2084, Dec. 2014.
- [6] F. Gabry, V. Bioglio *et al.*, "Multi-Kernel Construction of Polar Codes," *IEEE Int. Conf. Commun. (ICC)*, 2017.
- [7] P. Trifonov, "Chained Polar Subcodes," in *SCC 2017; 11th Int. ITG Conf. on Syst., Commun. and Coding*, Feb. 2017, pp. 1–6.
- [8] V. Bioglio, F. Gabry, and I. Land, "Low-Complexity Puncturing and Shortening of Polar Codes," in *2017 IEEE Wireless Commun. and Networking Conf. Workshops (WCNCW)*. IEEE, Mar. 2017.
- [9] M. Benammar, V. Bioglio *et al.*, "Multi-Kernel Polar Codes: Proof of Polarization and Error Exponents," *IEEE Info. Theory Workshop*, 2017.
- [10] G. Coppolino, C. Condo *et al.*, "A Multi-Kernel Multi-Code Polar Decoder Architecture," *IEEE Trans. on Circuits and Syst. I: Regular Papers*, pp. 1–10, 2018.
- [11] I. Tal and A. Vardy, "List Decoding of Polar Codes," *IEEE Trans. on Inform. Theory*, vol. 61, no. 5, pp. 2213–2226, May 2015.
- [12] G. Sarkis, P. Giard *et al.*, "Fast Polar Decoders: Algorithm and Implementation," *IEEE J. on Select. Areas in Commun.*, vol. 32, no. 5, pp. 946–957, May 2014.
- [13] G. Sarkis, P. Giard *et al.*, "Fast List Decoders for Polar Codes," *IEEE J. on Select. Areas in Commun.*, vol. 34, no. 2, pp. 318–328, Feb. 2016.
- [14] P. Trifonov, "Efficient Design and Decoding of Polar Codes," *IEEE Trans. on Commun.*, vol. 60, no. 11, pp. 3221–3227, Nov. 2012.
- [15] A. Cassagne, O. Hartmann *et al.*, "Fast Simulation and Prototyping with AFF3CT," in *Int. Workshop on Signal Process. Syst.* IEEE, Oct. 2017.
- [16] D. Wu, Y. Li, and Y. Sun, "Construction and Block Error Rate Analysis of Polar Codes Over AWGN Channel Based on Gaussian Approximation," *IEEE Commun. Letters*, vol. 18, no. 7, pp. 1099–1102, Jul. 2014.
- [17] C. Leroux, A. J. Raymond *et al.*, "A Semi-Parallel Successive-Cancellation Decoder for Polar Codes," *IEEE Trans. on Signal Processing*, vol. 61, no. 2, pp. 289–299, Jan. 2013.